

Study the Effect of Cutting Parameters on Temperature Distribution and Tool Life During Turning Stainless Steel 316L

Ahmed A. Akbar* Raed R. Shwaish** Naba D. Hadi***

*, **, ***Department of Production Engineering and Metallurgy Engineering/ University of Technology

*Email: akbarthree@yahoo.com

**Email: raedshuishe@gmail.com

***Email: nabaadhiyaa@gmail.com

(Received 19 September 2017; accepted 10 January 2018)

<https://doi.org/10.22153/kej.2018.01.007>

Abstract

This paper is focused on studying the effect of cutting parameters (spindle speed, feed and depth of cut) on the response (temperature and tool life) during turning process. The inserts used in this study are carbide inserts coated with TiAlN (Titanium, Aluminium and Nitride) for machining a shaft of stainless steel 316L. Finite difference method was used to find the temperature distribution. The experimental results were done using infrared camera while the simulation process was performed using Matlab software package. The results showed that the maximum difference between the experimental and simulation results was equal to 19.3 °F, so, a good agreement between the experimental and simulation results was achieved. Tool life was decreased when spindle speed and feed were increased.

Keywords: Cutting parameters, Finite difference method, Stainless steel 316L, Temperature distribution, Tool life, Turning operation.

1. Introduction

In metal cutting, amount of heat may be generated because of the friction at the tool-chip interface and plastic working of the solid. In the shear zone the metal is deformed plastically and removed in the form of chip [1]. The deformation of the material elasticity demand energy these energy was storing in a material like strain energy, and no amount of heat was formed while the material was deformation plastically, generally the energy that utilized was transform to heat. At cutting process a materials were undergo at large amount of strain and the deformation of materials elastically were form a tiny of the ratio of all deformation. It should be suppose all amount of energy was transformed to a heat [2]. agree with to the 1st rule of thermodynamics, while work was converted to a heat, the amount of a heat generated was equal to the amount of

work. Heat produced during transformation of mechanical energy. There are three sources of heat during metal cutting are given below [3] and shown in Fig. 1:

- 1.The shear zone, where the primary plastic or shear deformation takes place.
- 2.The chip-tool interface where secondary plastic deformation due to friction between the heated chip and tool takes place.
- 3.The work-tool. interface at flanks where frictional rubbing occurs (V_f).

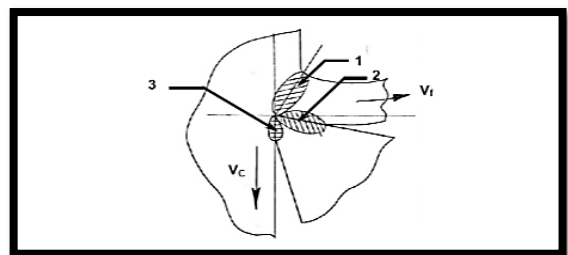


Fig. 1. Sources of heat in metal cutting [3].

Bartoszuk M. et al. [4] Studied finite difference method-based simulation of temperature fields for application to orthogonal cutting of AISI 1045 steel with coated tools. V. Astakhov et al. [5] Studied influence of cutting parameters on life of tool for AL 610 alloy, then showed that the best tool life is, obtained in lowest feed rate and lowest cutting speed combination. C. Dinc et al. [6] developed the effectiveness for formerly (finite difference time domain) temperatures predictions models was hold out to orthogonal cutting process by using (IR camera). In the cutting conditions using orthogonal machining of (Al 7075 and AISI 1050). Naife A. Talib [7] Studied, the influence of (speed of cut, and rate of feed), on life of tools at fixed cut depth for low alloy steel without cooling fluid. A maximum life was at maximum speed of cutting, (66.88) m/min and rate of feed (0.72) mm/rev, while the cutting tool life was (388.3) min. Sunday J. Ojolo and O. Ogunkomaiya [8] Studied the influence of cutting condition on life of tool using dry condition. They used 3 cutting tools material first (HSS), second tungsten carbide insert tool grade (P-10) (DMNG), and third carbide insert tool (150412-SA) and the workpiece material mild steel. Dhananchezian M. et al. [9] Studied of machinability properties for machining austenitic (AISI 316 L) and super duplex (2505) stainless steel utilizing (PVD-TIALN) nano-multilayer inserts. The effects of speed of cut on the temperatures, force of cut roughness of surface, wear of tool wear and chip breaking were analyzed. Oluseyi O. Ajayi et al. [10] Studied the development of thermo mechanical model for analysing effects of friction and cutting speed on temperature distribution during orthogonal machining of AISI 316 L.”

2. Temperature in the Shear Plane

Suppose in the shear plane zone:

1. The shear stress is constant (uniform),
2. The heat is generation within the work material and passing through the shear plane is uniform,
3. The work material when passing through shear zone is immediately and uniformly heated up.

The temperature of the work material is raises from the room temperature (T_r) to the shear-plane temperature (T_s). The temperature increase ($T_s - T_r$) is obtained by dividing the

shearing power, represents work (heat) in unit time, by the heat capacity of the material passing through the shear zone in unit time, which is the heat capacity of the metal removal rate Q [11]:

$$(T_s - T_r) = \frac{P_s}{Q \rho c} \quad \dots(1)$$

Where; P_s is shearing power (mW = Nmm/sec), ρ is specific mass (kg/m³), and c is specific heat (Nm/(kg . °C)).

The product (ρc) represents “the specific heat per unit volume” may be given by using the following units:

$$(T_s - T_r) \frac{P_s \text{ (Nmm/sec)}}{[bh(\text{mm}^2)v \text{ (mm/sec)} \rho c \text{ (N/(mm}^2 \text{ °C))}]}$$

Where; b is chip width (mm), v is cutting speed (mm/sec), and h is chip thickness (mm).

$$P_s = F_t V_s = \frac{F_t}{\cos \beta} \frac{\cos(\beta + \phi) v}{\cos \phi}$$

Let us denote

$$D = \frac{\cos(\beta + \phi)}{\cos \beta \cos \phi}$$

Then

$$P_s = F_t v D = K_s b h v D$$

$$T_s - T_r = \frac{K_s b h v D}{b h v \rho c} = \frac{K_s D}{\rho c} \quad \dots(3)$$

Where; K_s is Specific force (N/mm²).

The shear-plane temperature proportional to the (K_s) and inversely proportional to specific mass ρ and specific heat c . In this way, (T_s) is determined by the mechanical and thermal properties of the workpiece only and it applies even to very slow cutting. While the power spent in the shear plane increases with chip thickness and speed, the flow rate of material through the plane that gets heated by that power increases in the same proportion. Actually, because (K_s) slightly decreases with chip thickness h , and cutting force F further decreases with cutting speed (v), the shear-plane temperature partially decreases with the increase of both (h) and (v). In the chip tool interference that seen in Fig. 2, the friction power is generated and it is distribution at a region linked, among a tool and a chips, that seen in Fig. 2, the distribution of friction energy followed the normal pressure distribution of. In the numerical treatment we divide the chip into number of elements both in two direction. The (X) direction of the face of the tool and the (Y) direction of the shear plane. The subscript for the former division is denoted K , and it starts with cutting edge where ($K = 1$) to the end, of the contact length (L_c) where ($K=KK$) [11]. The tool pressure founded experimentally maximum & constant over the

distance ($h_1/2$) from, the cutting edge and decrease linearly between this point and the end of contact [12]. The friction (P_f) power can derive acting over the area ($b\Delta x$) of the one slice. Assume that the length of contact is proportional to the undeformed chip thickness (h_1) [11].

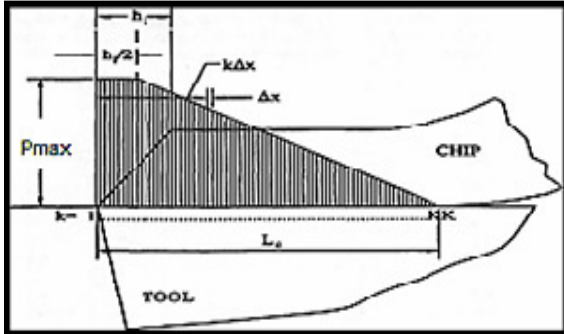


Fig. 2 . Distribution of friction power over the rake face of the tool [11].

$$L_c = mh_1$$

m : Number shows the amount of amplification.

Then

$$\frac{h_1}{2} = \frac{L_c}{2m} = \frac{KK}{2m} \Delta x \quad \text{And}$$

$$P_{max} \left[\frac{KK}{2m} + \frac{1}{2}KK \left(1 - \frac{1}{2m} \right) \right] = P_f \quad \dots(4)$$

*For $K \leq KK/2m$, $P_k = P_{max}$

*For $\frac{KK}{2m} < K \leq KK$

$$P_k = P_{max} - \Delta P \left(K - \frac{KK}{2m} \right) \quad \dots (5)$$

Where

$$\Delta P = \frac{P_{max}}{KK(1-1/2m)} \quad \dots(6)$$

*For $K > KK$, $P_k = 0$

3. Computing the Temperature Field:

The computing of temperature field are divided in two phase [11]:

3.1. Phase 1: Neglecting Heat Escaping Through the Tool:

The heat convected of chips to the rounded air was suppose totally ignored, and never heat was conduction far away during the tool. A former assumption is quite realistic, while the latter introduced that will be computed and corrected in Phase

2.Both these assumptions mean that all heat is conducted away by the chip.

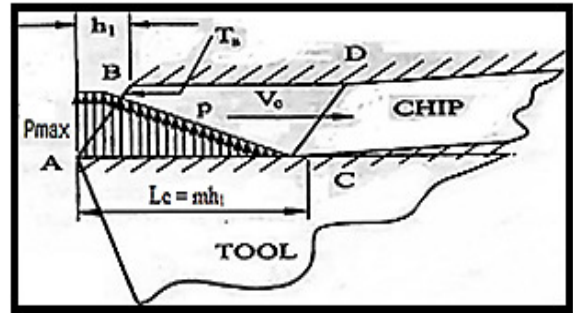


Fig. 3. a. The area of chip[11].

Fig.3.a shows the area of chip ABCD. The boundary conditions are along the AB shear plane the temperature is (T_s), along AC and BD the chip is insulated, and along AC above (L_c) where the (heat) inter because of the friction at chips-tool. The amount of force of friction and, the heating power are distributed as shown: it founded constant and maximum from the edge of cutting a along one over two the thickness of undeforming chips (h_1) & then it lowering straightly towards the ending of a linked. Heat spreads onto a chips using conductions and transfer of mass at orientation (X) and using conductions only at orientation (Y).

The whole field of the chip is divided into incremental slices in the two directions. In direction X are subscripted K, from (1 to KK) above length of contacts and up to a total of KKK. The slices in the direction Y are subscripted from 1 to 20 by this way, the whole field is divided into 20 times KKK elements. By using the method of finite differences, we suppose a temperatures was fixed along all parts and alteration discretely for part to next part.

Boothroyd [2] found that mass transfer of heat in X is much more powerful than conduction. The latter can be neglected; it is sufficient to consider the former mode only. Correspondingly, we will consider heat conducted in Y direction and, heat moved by mass transfer in X direction. This is symbolically expressed by assuming that every vertical slice moves in direction X with the chip velocity (v_c) while being insulated, in direction X, against the neighboring slices, as shown in Fig.3.b, for the (K_{th}) slice. Instead of considering a steady-state, two-dimensional (X,Y) heat transfer problem we formulate one-dimensional (Y) transient case. We will follow one vertical slice as it moves, in discrete increments of time, through positions from 1 to KKK. Above the (L_c), for (1 to KK) its obtain on it minimize ending the (P_k) & the generated

heats was diffusion in these slices at orientation (Y), by conduction. Between KK and KKK there is no more heat input. The temperature of every element $T_{j,K}$ varies through the steps 1 to KKK. Under the assumption of no convection of heat out of the chip, the temperature in such a slice, far away from the end of the. contact zone, would approach a uniform, constant value. For practical purposes we choose the following. equation:

$$KKK = \frac{3KK}{2} \dots(7)$$

The shear-plane temperature is found by using Eq. (2), It will further be accepted that on average for most our demonstrations ($L_c = 4h_1$). The total heat flow over the area of the contact length (L_c) times the chip width (b) equals the friction power (P_f).

$$P_f = F_f \cdot v_c$$

Where; F_f is the friction force.

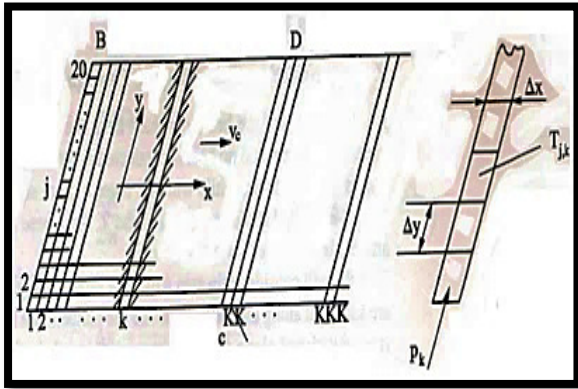


Fig. 3.b. Finite-difference formulation for temperatures in the chip [11].

The heat flux distribution is as shown in Fig.2, and it is expressed in Eq. (4), (5), and (6) in the form of the power injected into each slice. The primary states of thermal fields onto the chips was like that in the slice where $K = 1$ have the uniform shear-plane temperature:

$$T_{j,1} = T_s \quad \text{where } j = 1 \text{ to } 20 \quad \dots(8)$$

The lowest element $j=1$, at every instant K receiving input heat (P_k) and losing heat by the conduction to neighbor part ($j = 2$). excess heats was using for increased temperatures along (Δt) times instant for ($T_{1,K} - T_{1,K+1}$)

$$P_k - \left(\frac{T_{1,K} - T_{2,K}}{\Delta y} \Delta x b k' b \Delta x \Delta y \rho c \frac{T_{1,K+1} - T_{1,K}}{\Delta t} \right) \dots(9)$$

$$\Delta t = \frac{\Delta x}{v_c} = \frac{L_c}{KK v_c} \dots(10)$$

The “conducted heat per time step Δt from $j = 1$ to $j = 2$ is considered the second

expression in the bracket on the left side of Eq (9)”. It was relative for a temperatures gradients [$(T_{1,K} - T_{2,K})/\Delta y$], for region [$A = \Delta x b$] & for the (k') (thermal conductivity). The rights direction was (ρc) (heat capacity of parts). For element $j = 2$ to 19, in state heat input P_k the inflow of heat for following minimize part was using:

$$\left(\frac{T_{j-1,K} - T_{j,K}}{\Delta y} - \frac{T_{j,K} - T_{j+1,K}}{\Delta y} \right) \Delta x b k' = b \Delta x \Delta y \rho c \frac{T_{j,K+1} - T_{j,K}}{\Delta t} \dots(11)$$

For, ($j = 20$) a second expression at left side of Eq. (11), was missing in order to heat was no conduction far away from part and no convection of heat far away the chips. Eqs. (9) to (11) using to expression a temperature for times [$(K+1)$]:

$$T_{j,K+1} = \begin{cases} \left[\frac{P_k}{b \Delta x \Delta y \rho c} - \frac{(T_{1,K} - T_{2,K}) \alpha}{(\Delta y)^2} \right] \Delta t + T_{1,K}, & j = 1 \\ (T_{j-1,K+1} + T_{j+1,K} - 2T_{j,K}) \frac{\alpha \Delta t}{(\Delta y)^2} + T_{j,K}, & j = 2 - 19 \\ (T_{19,K+1} - T_{20,K}) \frac{\alpha \Delta t}{(\Delta y)^2} + T_{20,K}, & j = 20 \end{cases} \dots(12)$$

where $\alpha = k'/\rho c$. In Eqs. (12) the first expression on the right side of equations is subscripted ($K + 1$) and not K as could have been expected. This means that we are updating the temperature as soon as the new values of temperature are available, which lead to improves the convergence and stability of the calculation. The increment in time Δt , Eq. (10), shouldn't be selected much large in order to the calculation in separated steps shouldn't converge. This leads to a minimum value of KK for computational stability.

3.2. Phase 2: Correcting for Heat Escaping Through the Tool:

The shape of the tool and the thermal field in it are strongly simplified, see Fig.4, as follow:

Heat is generated first in shear plane (S) and then in the chip/tool contact. Most of it is taken away by the chip, but some of heat flows through tools to the tools holder, and into the machine parts. It is assumed that:

- Amount of generated heat was convect and radiate through a tool onto air, then heat escaping into the air is neglected.
- The tool escape from the area of cut was already at back ground temperature.
- The isotherm at tools were upper or lower line for the equivalent displacement for the area of cutting. Thus we will represent tools

as a dowel within a (chips/tools) linked region at a roof apex. It should be spilt on slices within thickness. (Δz_i), depth (b) (into the paper), and width (w_i).

- The thermals fields was a 1-dimension at (z), however each slice have a fixed temperatures everywhere.
- While the bed (bottom) was at background temperatures (T_r) and sides were isolated. For the points of vision of tools the heat over the (L_c) was fixed. It should been possessed as equivalent to the rate of temperatures above contact length (L_c).

So we formulate a fixed (steady-state), (1-dimensional) problem. The temperature T_{cav} is expressed in the equation below:

$$T_{cav} = \frac{1}{KK} \sum_1^{KK} T_{1,K} \quad \dots(13)$$

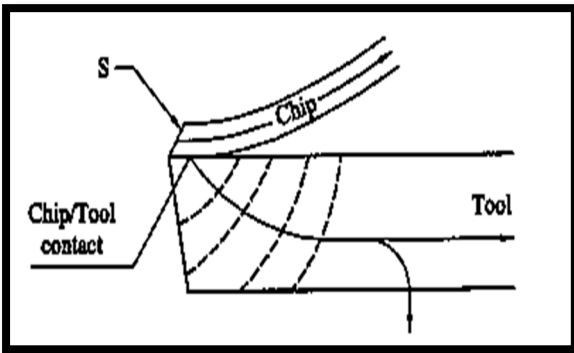


Fig.4.a: The general set up [11].

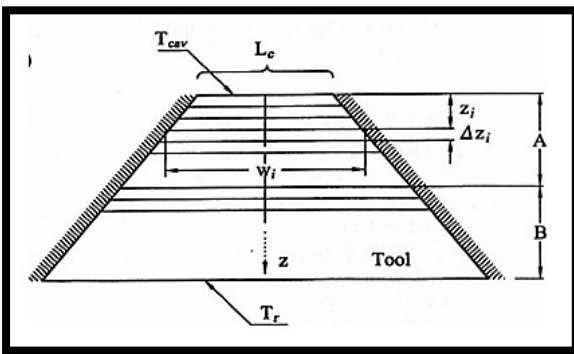


Fig. 4.b. The finite-difference formulation Diagram of the tool [11].

The temperatures (T_i) of the individual slices do not change (steady state). All heat that entering the slice departure the slice. A power flux during a tools was (P_t) & it was similar for all slices shown in Fig. 5. The 1st step starts from the tool top (the linked among the tool and the chips) and then to middle of the slice top when temperature (T_i), was location. The means width was equal:

$$w_1 = L_c + \frac{\Delta z}{2} \quad \dots(14)$$

For whole a following slices, we move from the slice middle to the next one middle distance is Δz , & (w_i) was equal by taken a together 40 layers:

$$w_i = L_c + 2(i - 1) \Delta z, \quad (i = 2-40) \quad \dots(15)$$

a final slices stage leave for ($T_{40} - T_r$) at a distance of ($\Delta z/2$):

$$w_{41} = L_c + 79.5 \Delta z \quad \dots(16)$$

Then we have

$$P_t = \frac{T_{cav} - T_1}{\Delta z/2} \times w_1 b k'_a, \quad R_1 = \frac{\Delta z/2}{w_1}$$

$$P_t = \frac{T_1 - T_2}{\Delta z} \times w_2 b k'_a, \quad R_2 = \frac{\Delta z}{w_2}$$

$$P_t = \frac{T_1 - T_{i+1}}{\Delta z} \times w_i b k'_i, \quad R_{i+1} = \frac{\Delta z}{w_{i+1}}$$

$$P_t = \frac{T_{41} - T_r}{\Delta z/2} \times w_{41} b k'_b, \quad R_{41} = \frac{\Delta z/2}{w_{41}} \quad \dots(17)$$

Where: k'_a is thermal conductivity of tool.

Now, expressing the individual temperatures in terms of T_{cav}

$$T_1 = T_{cav} - \frac{P_t}{b k'_a} R_1$$

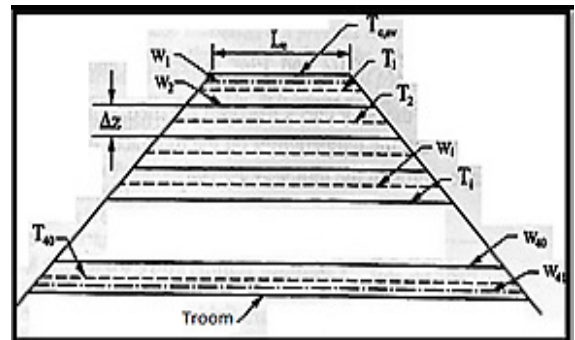


Fig. 5. Specification of die thermal field in the tool as steady-state single-dimensional [11].

$$T_2 = T_1 - \frac{P_t}{b k'_a} R_2 = T_{cav} - \frac{P_t}{b} \left(\frac{R_1}{k'_a} + \frac{R_2}{k'_a} \right) \dots(18)$$

$$T_{i+1} = T_i - \frac{P_t}{b k'_i} R_{i+1} = T_{cav} - \frac{P_t}{b} \sum_1^{i+1} \frac{R_i}{k'_i} \dots(19)$$

$$\text{Denoting } r = \sum_1^{41} \frac{R_i}{k'_i} \quad \dots(20)$$

$$T_r = T_{cav} - \frac{P_t r}{b}$$

and

$$P_t = (T_{cav} - T_r) \frac{b}{r} \quad \dots(21)$$

The "thermal resistance" r can be calculated by the dimensions and thermal conductivities of the tool.

4. Experimental Work

The experimental work were done by using universal turning type sinus 330/3000. (SN-126130). The inserts used in this paper is carbide inserts coated with TiAlN. Fig.6 shows the machining operation and temperature measurement.



Fig. 6. Workpiece on the machine and temperature measurement using fluke camera.

4.1 The Workpiece Material

The workpeice material is a shaft of stainless steel 316 L, which is inspected in Central Organization for Standardization and Quality Control / lab. of quality control. The chemical composition and thermal properties are shown in tables (1) (2) respectively. The stainless steel shaft has diameter (74) mm.

Table 1, Chemical composition of stainless steel 316L.

| metal | wt% | metal | wt% |
|-------|--------|-------|---------|
| C% | 0.0044 | Cu% | 0.597 |
| Si% | 0.432 | Cr% | 18.2 |
| Mn% | 1.74 | Mo% | 2.19 |
| P% | 0.0271 | S% | 0.0216 |
| Ni% | 9.55 | Fe% | Balance |

Table 2, Thermal properties of stainless steel 316L and tool [13].

| Property | Values | Unit |
|--|--------|-----------------------------|
| Thermal Conductivity of workpiece (k) | 16.3 | (W/m.°k) |
| Specific Electrical Resistivity | 0.75 | Ω mm ² /m |
| Specific heat at 20 c° | 3.6 | N/(mm ² .°C) |
| Thermal diffusivity | 3.9 | m ² /s |
| Specific force | 2600 | N/mm ² |
| Thermal Conductivity of carbide insert k_a | 70 | N/S. °C |
| Thermal Conductivity of tool shank k_b | 43 | N/S. °C |

4.2 Temperature Measurement

All temperature measurement were tested using (IR- Camera fluke) shown in Fig. 7. The cutting parameters and experimental result of temperature are shown in table 3. The IR Camera need some set before making the measurement like (emissivity, background temperature, time, date). The emissivity of any material was value of irradiation whose emanate proportional to the (pure black body). The black body was typical motive and a typically absorption as well. The emissivity value was (0 to 1). The emissivity of a black body is (1) [14]. In this work the emissivity value is (0.05) and the value of background temperature is (30°C).



Fig. 7. IR-Camera fluke

Table 3, Cutting parameters and experimental results of temperature.

| Spindle speed (r.p.m) | feed (mm/rev) | Depth of cut (mm) | Temperature (°F) |
|-----------------------|---------------|-------------------|------------------|
| 400 | | | 843.1 |
| 500 | 0.1 | 0.5 | 930 |
| 630 | | | 943.4 |
| 800 | | | 957.5 |
| 1000 | | | 1031.1 |
| | 0.1 | | 843.1 |
| | 0.12 | | 941.8 |
| 400 | 0.14 | 0.5 | 961.6 |
| | 0.16 | | 977.5 |
| | 0.18 | | 980.7 |
| | | 0.5 | 843.1 |
| | | 0.7 | 915.1 |
| 400 | 0.1 | 0.9 | 960 |
| | | 1.1 | 966.3 |
| | | 1.3 | 995.6 |

4.3 Tool Life Calculation

Tool life can be calculated by using taylor equations. The cutting parameters and experimental result of tool life are shown in table 4. The value of constant (Ct and nt) can be

calculated by using graphical methods as shown in Fig.8.

$$-nt = -1.4938$$

$$\text{Log Ct} = 3.8253$$

$$Ct = 6688.05$$

Use taylor equation to find tool life [15]

$$V_c \times T^{nt} = Ct \quad \dots(22)$$

$$T = 17.95 \text{ min}$$

Where: Ct is constant and nt is exponent that depends on the cutting parameters.

The equation used to find cutting speed shown below [16]:

$$V_c = \frac{\pi DN}{1000} \quad \dots(23)$$

Where: V_c is cutting speed (m/min), N is spindle speed (r.p.m), and D is work diameter (mm).

Table 4,
Cutting parameters and experimental results of tool life.

| Spindle speed (r.p.m) | feed (mm/rev) | Depth of cut (mm) | Tool life (min) |
|-----------------------|---------------|-------------------|-----------------|
| 400 | | | 17.95 |
| 500 | 0.1 | 1.1 | 15.45 |
| 630 | | | 13.27 |
| 1000 | | | 9.75 |
| | 0.1 | | 17.95 |
| 400 | 0.12 | 1.1 | 17.4 |
| | 0.14 | | 17.26 |
| | 0.18 | | 16.98 |

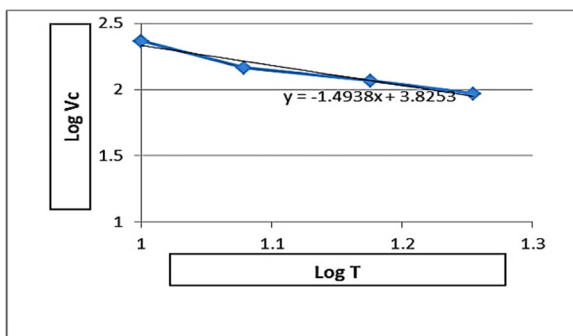


Fig. 8. Graphical method.

5. The Results and Discussion

5.1 The Effect of Cutting Parameters on Temperature

The effect of spindle speed on the temperature shown in Fig.9, It can be seen with increase the spindle speed the maximum temperature increase. The reason is when the spindle speed increase, the strain rate in the primary and secondary shear zone increased so the heat flux generated and cause the increase.

The effect of feed on the temperature shown in Fig.10. It can be seen with increase the feed the maximum temperature increase. The reason is the increase in the feed lead to increase the cross section of chips so the friction increase and making the increase in the maximum temperature.

The effect of depth of cut on the temperature shown in Fig. 11, It can be seen with increase the depth of cut the maximum temperature increase. The reason is when depth of cut increase the cross section of chip increase and lead to increase the friction so the temperature increase.

5.2 The Effect of Cutting Parameters on Tool Life

The effect of spindle speed on tool life shown in Fig. 12, The tool life decrease when the spindle speed increase. The reason is when spindle speed increased the tool wear increase, and cutting time decrease lead to decrease tool life.

The effect of feed rate on tool life shown in Fig. 13, The tool life decrease when the feed rate increase the reason is when feed rate increase the amount of heat generated is increase so the cutting tool is subjected to quick collapse lead to decrease the tool life.

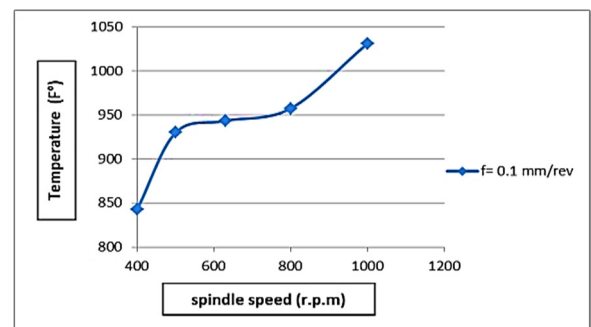


Fig. 9. Effect of spindle speed on temperature.

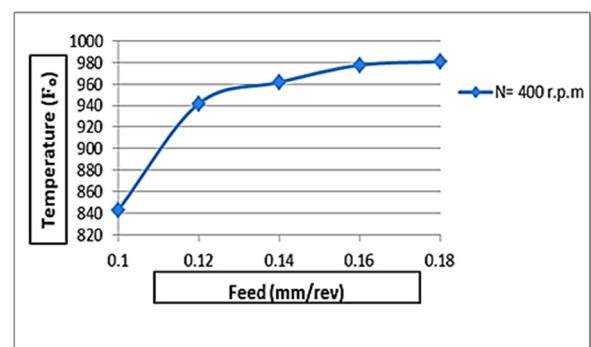


Fig. 10. Effect of feed on temperature.

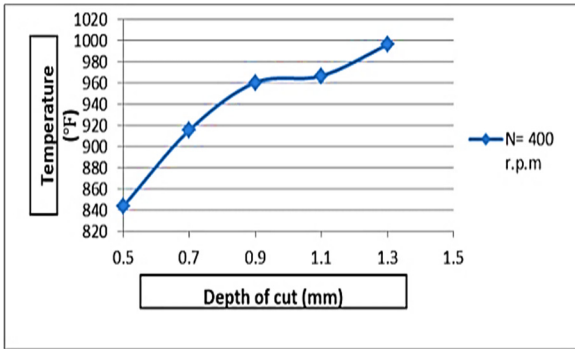


Fig. 11. Effect of depth of cut on temperature.

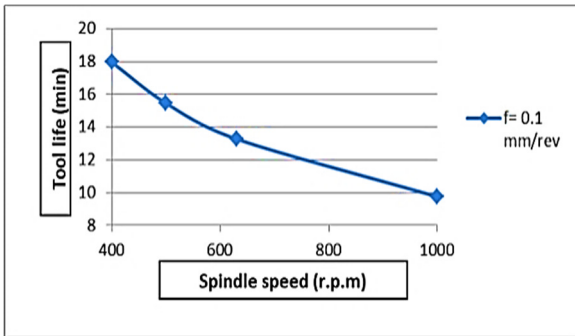


Fig. 12. Effect of spindle speed on tool life.

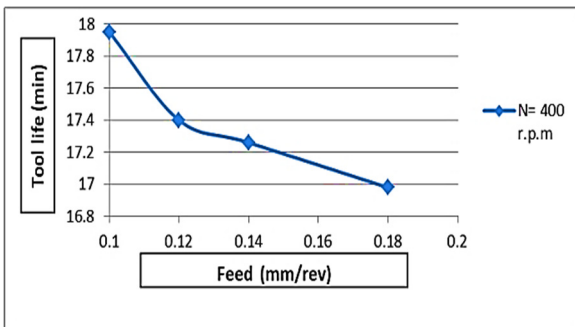
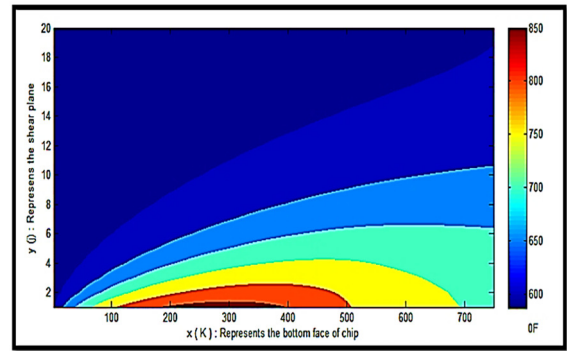


Fig. 13. Effect of feed on tool life.

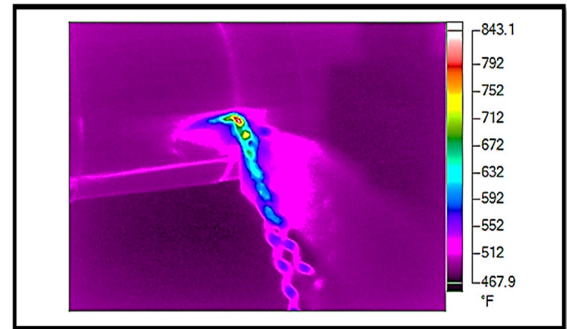
5.3 The Comparison Between the Experimental and Simulation Results of Temperature.

The experimental result obtained from (IR-Camera). The thermal image are produced by using smart view software version (3.1). high contrast colors scales was fitted to a picture. A simulation result produced by using Matlab program to draw the temperature distribution using contour plot. The difference between experimental value and simulation value is

$$\text{Difference} = \text{experimental value} - \text{simulation value}$$

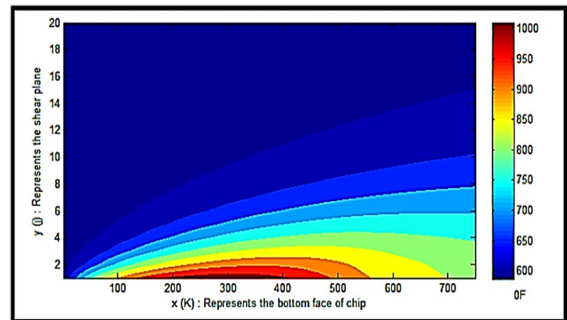


(a)

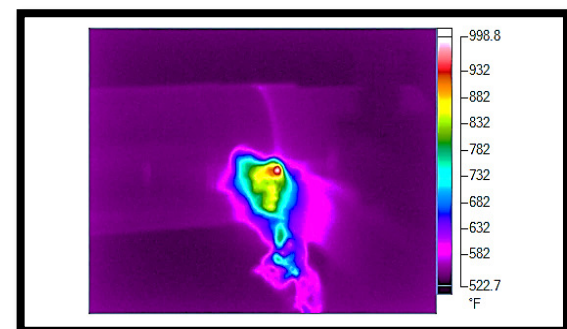


(b)

Fig. 14. Temperature fields of machining with spindle speed (400 r.p.m), feed (0.10 mm/rev), depth. (0.5m), (a) temperature distribution simulation, (b) experimental measuring of temperature using IR-Camera.

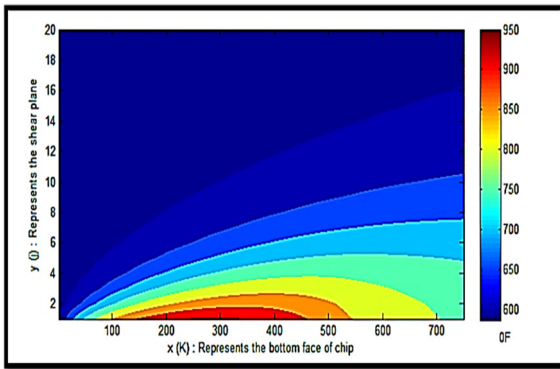


(a)

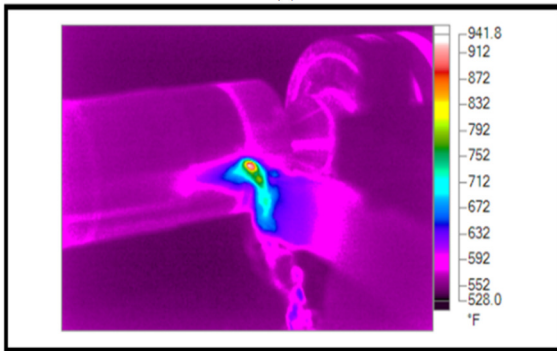


(b)

Fig. 15. Temperature fields of machining with spindle speed (500r.p.m), feed (0.1mm/rev), depth (0.5mm), (a) temperature distribution simulation, (b) experimental measuring of temperature using IR-Camera.

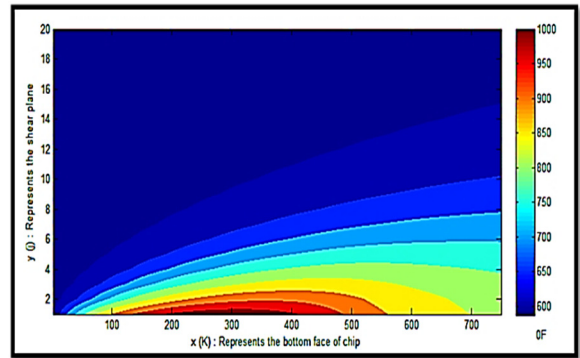


(a)

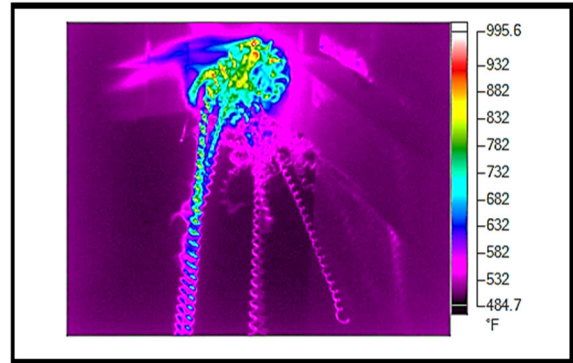


(b)

Fig. 16. Temperature fields of machining with spindle speed (400 r.p.m), feed (0.12 mm/rev), depth (0.5 mm), (a) temperature distribution simulation, (b) experimental measuring of temperature using IR-Camera.

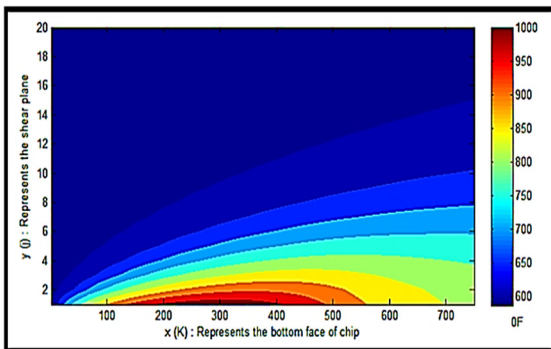


(a)

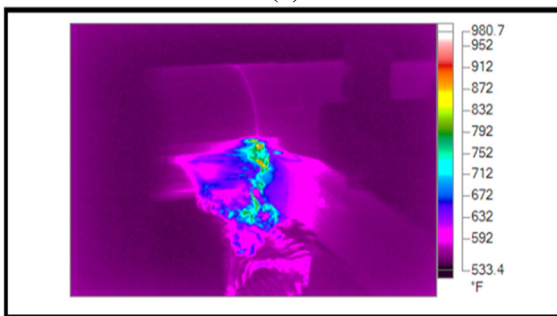


(b)

Fig. 18. Temperature fields of machining with spindle speed (400 r.p.m), feed (0.10mm/rev), depth (1.3 mm), (a) temperature distribution simulation, (b) experimental measuring of temperature using IR-Camera.



(a)



(b)

Fig.17. Temperature fields of machining with spindle speed (400 r.p.m), feed (0.18 mm/rev), depth (0.5 mm), (a) temperature distribution simulation, (b) experimental measuring of temperature using IR-Camera.

6. Conclusions

The main concluded of the present work are the following

1. IR-Camera is the best way to measure the temperature because it is easy to install and give the result with good accuracy".
2. The relationship between the maximum temperature and tool life, when the temperature increase the tool life decrease.
3. The maximum temperature of stainless steel AISI 316L is (1031.1°F) at spindle speed (400 r.p.m), feed (0.1 mm/rev), depth of cut (0.5 mm).
4. The maximum difference between the experimental value and simulation value is (19.3°F). So the results shows a good agreement with the simulation value.

7. References

- [1] T. D. Marusich, M. Ortiz, "Modeling and Simulation of High - Speed Machining", International Journal Numerical Methmatical Engineering, vol. 38, 1995, Pp. 3675-3694.
- [2] Boothroyd, G., "Fundamentals of Metal Machining and Machine Tools" International Student Edition, Mc Graw Hill International Book Company Tokyo, 1981, Pp.109.
- [3] A. Bhattacharyya, I. Ham, "Design of Cutting Tool Use a Metal Cutting Theory, 1st edition, astme p. committee, 1969, Pp. 347.
- [4] M. Bartoszuk, W. Grzesik, P. Neslony, "Finite Difference Method-Based Simulation of Temperature Fields For Application To Orthogonal Cutting", International Journal of Machining Science and Technology, vol.9, issue 4, 2005, Pp. 529-546.
- [5] V. Astakhov, "Effects Of The Cutting Feed, Depth of Cut, and Workpiece (Bore) Diameter on The Tool Wear Rate," International Journal of Advanced Manufacturing Technology, vol. 34, issue 7-8, 2006, Pp. 1-10.
- [6] C. Dinc, I. Lazoglu, A. Serpenguzel, "Analysis of Thermal Fields In orthogonal Machining With Infrared Imaging", Jornal Of Materials Processing Technology, vol. 98, 2008, Pp.147- 154.
- [7] Naife A. Talib, "Studying The Effect of Cutting Speed and Feed Rate on Tool Life In The Turning Processes", Diyala Journal of Engineering Sciences, special issue, 2010, Pp.181-194.
- [8] Sunday Joshua Ojolo and Olugbenga Ogunkomaiya," A Study of Effects of Machining Parameters on Tool Life", International Journal of Materials Science and Applications. Vol. 3, No. 5, 2014, Pp. 183-199.
- [9] Dhananchezian M. Thinesh T, Steven Niketan Paul and Inian Roy A, "Study Of Machinability Characteristics For Turning Austenitic (316L) And Super Duplex (2505) Stainless Steel Using Pvd-Tialn Nano-Multilayer Inserts", ARPN journal of engineering and applied sciences, vol.11, No.2, 2016.
- [10] Oluseyi O. Ajayi, Abatan Abiola, Mercy Ogbonnay, Agarana Michael, "Development of Thermomechanical Model For Analysis of Effect of Friction and Cutting Speed on Temperature Distribution Around AISI 316 L During Orthogonal Machining", international conference on sustainable materials processing and manufacturing, 2017, Pp. 682-687.
- [11] George Tlusty, "Manufacturing Process and equipment", first edition, 2000, prentice hall.
- [12] A. and yellowley I. , "process detection of tool failure in milling using cutting force model", Journal of manufacturing science and engineering", 1989, 111(2), Pp. (149-157).
- [13] www.Stainless steel 316L
- [14] V. Dessoly, "Modeling and Verification of Cutting Tool Temperatures In Rotary Tool Turning of Hardened Steel", master thesis, Mechanical Engineering, Georgia Institute of Technology, 2004. Pp.(67).
- [15] J. Paulo Davim, "Machining of Hard Materials", Springer-Verlag London Limited, 2011, Pp.54.
- [16] M. P. Groover, "Fundamentals of Modern Manufacturing", third edition, lehigh university, 2007, Pp. 509.

دراسة تأثير □ على □ لآت التشغيل على توزيع درجة الحرارة وعمر الاداة اثناء تشغيل الفولاذ المقاوم للصدأ 316L

احمد علي اكبر * رائد رشيد شويش** نبع ضياء هادي***

،،*** قسم هندسة الانتاج والمعادن/ الجامعة التكنولوجية

* البريد الالكتروني: akbarthree@yahoo.com

** البريد الالكتروني: raedshuishe@gmail.com

*** البريد الالكتروني: nabaadhyyaa@gmail.com

الخلاصة:

يرتكز هذا البحث على دراسة تأثير معاملات التشغيل مثل (سرعة الدوران و التغذية و عمق القطع) على الاستجابة (درجة الحرارة) (عمر الاداة) اثناء عملية الخراطة. اللقمة المستخدمة هي لقمة كربيدية مصبوغة بـ (Titanium Aluminum Nitride) (TiAlN) لتشغيل عمود الفولاذ المقاوم للصدأ 316 L. طريقة الفرق المحدد استخدمت لاجاد التوزيع الحراري. النتائج التجريبية تمت باستخدام كاميرا الاشعة تحت الحمراء وعملية المحاكاة تمت باستخدام برنامج ماتلاب. النتائج بينت ان اعظم فرق بين النتائج التجريبية والمحاكاة هي (19.3°F). لذلك اظهرت توافقاً جيداً بين النتائج التجريبية والمحاكاة. عمر الاداة تقل بزيادة سرعة القطع والتغذية.